Optics Letters

Influence of atmospheric helium on secondary clocks

Ko-Han Chen,[1,2,3] Chien-Ming Wu,[1,3] Shu-Rong Wu,[1] Hsin-Hung Yu,[1] Tze-Wei Liu,[1,2,3] and Wang-Yau Cheng[1,2,*]

[1]Department of Physics, National Central University, Taoyuan City 32001, Taiwan
[2]Molecular Sciences and Technology, Taiwan International Graduate Program, Academia Sinica, National Central University, Taipei, Taiwan
[3]Institute of Atomic and Molecular Science, Academia Sinica, Taipei 11529, Taiwan
*Corresponding author: Wycheng@phys.ncu.edu.tw

Received 6 April 2020; revised 22 May 2020; accepted 8 June 2020; posted 9 June 2020 (Doc. ID 394464); published 15 July 2020

Glass-cell–based secondary clocks, including coherent population trapping (CPT) clocks, are the most used clocks in modern laboratories and in industry. However, the reported frequency accuracies of those secondary clocks were always much worse than expected, though all error sources have been previously discussed. In this report, a high-precision measurement on the spectral frequency-linewidth relation (FL-R) is first used for revealing a new error source in secondary clocks by which we answer the puzzle raised in Opt. Lett. 38, 3186 (2013). © 2020 Optical Society of America

https://doi.org/10.1364/OL.394464

Without secondary standards (clocks), the definition of the "second" would encounter difficulty to be generally achievable [1] because the conditions for both laser operation and frequency accuracy dissemination of the primary standards are stringent. Hence, secondary clocks play a key role in space voyages, length-standard related metrology, and the time base of advanced instruments, among other applications. Most secondary clocks are created with glass cells because of their high stability and compactness [2–16]. Yet, the frequency accuracy of atomic transitions determined from intercomparisons or "absolute frequency" measurements have always been of a lower quality than expected, which has puzzled metrologists for decades [15]. For instance, the laser frequency instability of rubidium (Rb) atom 5S–5D [5–7] and 5S–7S [8–12] hyperfine-transition–based clocks can reach values of 10^{-13} to 10^{-14} (fractional: $\Delta f/f$), but independent laboratories have only reported laser frequencies with an agreement of 10^{-11} to 10^{-12} [3,4,6,7,11]. A similar situation also arose in cesium (Cs)-cell–based 6S–8S two-photon transitions: in 2007, Hansch's group reported an inaccuracy of 10^{-11} compared with the result of Biraben's group [13,14]. The accuracy of these measurements hinges critically on collision-based frequency shifts which were only estimated in those publications. After we examined 11 cells from 2013 to 2015 [15,16], we observed that the transition frequencies differed by as much as 400 kHz, which surprised metrologists and led to suspicion of all previous secondary standards, as mentioned in Ref. [15]. In 2014, Zameroski *et al.* [17] raised a thought-provoking hypothesis: our previous results [15] might have been due to collisions of helium (He) originating from the atmosphere. Proving this hypothesis is challenging because the atmosphere contains only 4 mTorr [17] of He and the diffusion time is too long to perceive the He penetrating. In our previous experiments [15,16], we developed a spectroscopic technology that enabled us to accurately determine the "frequency-linewidth" relation (FL-R) of atomic transition while maintaining the laser highly stabilized, which is the key technology in this Letter for unveiling a new error source of secondary clocks. In this Letter, we report three independent experiments conducted to demonstrate the significance of the spectral FL-R, with the use of the Cs 8S-level as a sensitive indicator. Our experimental data support the hypothesis proposed in Ref. [17] and hence solves the conundrum mentioned in Ref. [15].

Figure 1 illustrates our optical layout for calibrating the master laser frequency by comb laser and for cesium spectrometers comparisons. The main principle and the experimental details have been described in Refs. [15,16]. Only two arrangements are different: one is that, in here, the electro-optical modulator (EOM) sideband does not pass cell #1 twice. Therefore, the crossover resonances are not influenced by quantum interference. The symbol $S_i (i = 1, -1, 2, -2)$ in Fig. 1 stands for the two-photon spectrum resolved by i-th sideband; C_{ij} stands for the crossover between carrier (i, $j = 0$) and sideband (i, $j = 1, 2$) [16]; the other difference is the implementation of additional vacuum chambers. All Cs cells used in Fig. 1 were examined at room temperature to minimize the Cs–Cs self-collision shift to negligible levels [15], except for cell #1 (90°C) that was used for laser stabilization. The frequencies mentioned in this Letter were all reference to a Cs microwave standard [18]. The two Cs spectrometers were intentionally constructed to be nearly identical and the Pyrex-made Cs #2 and Cs #3 have nearly the same dimensions, with which we have once measured the transition frequencies in 2012 and 2017. After measuring the 6S–8S transition frequencies, we placed the Cs #3 inside a vacuum chamber filled with 1.75 atm He gas, as shown in Fig. 1, to real-time monitor the He diffusion process. Subsequently, the whole He-chamber system was replaced by

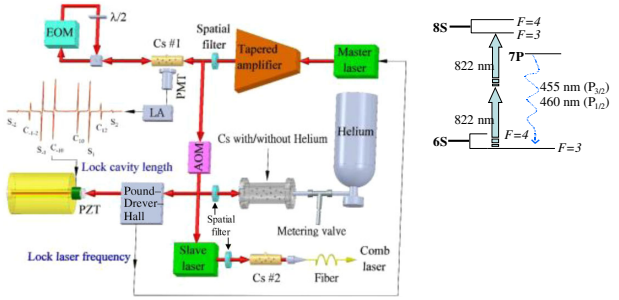

Fig. 1. Simplified diagram of the experimental setup for observing the He collision shift of Cs 6S–8S transition. LA, lock-in amplifier; upper right, relevant level diagram in the Cs atom. See text for the upper-left derivative spectrum (transverse axis: laser frequency).

another Cs-dispenser–based vacuum chamber to study the He–Cs collision and to determine the "ultimate absolute" Cs 6S–8S transition frequency in a background vacuum of 10^{-8} Torr. Table 1 lists the frequencies of Cs atom $6S \rightarrow 8S$ hyperfine transition measured from four independent Cs sources in which the "cell #4" stands for the narrowest-linewidth cell examined in 2012 [15]. The light shifts, pressure shifts, Zeeman shifts and other error sources were all considered in the same manner as in our previous works of determining the frequencies [15]. The linewidths in this paper were all fitted using a convolution of Lorentzian and transit-time broadening [19] and are referred to as "Lorentzian-transit" here. Under the Lorentzian-transit fitting, we find that the four Cs sources in Table 1 resulted in the same transit-time broadening of 365 (5) kHz since the spectra were all measured with nearly the same laser beam size. The phrase "vacuum cell" in Table 1 refers to a Pyrex cell that was connected to a high-vacuum chamber (1×10^{-8} Torr). The data presented in Table 1 are highly correlated. For example, the frequency discrepancies of the $F = 4$ transition between different cells were the same as those for the $F = 3$ transition, and the hyperfine intervals measured with different cells were all the same within our measurement uncertainty, which means that the diverse absolute frequencies obtained from different Cs cells were not caused by measurement errors.

Moreover, during the 5 years, the frequency shifts and the amount of line broadening of the $F = 4 \rightarrow F' = 4$ transition in cell #2 and cell #3 were almost the same, despite these cells being purchased from different companies in separate years. After completing all the measurements displayed in Table 1, we gradually introduced He into a 10^{-8} Torr vacuum chamber. The vacuum was constantly monitored using a wide-range gage, which was previously calibrated [20]. The inset of Fig. 2 indicates how sensitive the lineshape of the Cs 8S hyperfine level was to the collision of the He partner [21]. Figure 2 depicts the linearity of the collision shift verses the He pressure. Notably, the blue shift feature of the collision partners of light molecule, like He and hydrogen (H_2), were unique among the possible outgassing molecule partners [17,22], whereas the collision of H_2 yields a different frequency-pressure slope than that of He [22]. This is because different scattering cross section are uniquely characterized by the different electron configurations of molecules, which will lead to different ratio of the elastic dipole scattering (frequency shift) to the inelastic quenching collision (lineshape broadening) [21,22]. The frequency shift in Fig. 2 provides crucial information regarding how to determine the amount of helium pressure in a suspicious Cs cell whenever the Cs collision partner has been confirmed to be He. Moreover, the FL-R in Fig. 3 offers further critical information for identifying whether the collision partner in a Cs cell is He or not and includes all the cells displayed in Table 1. We find, surprisingly, that the FL-R derived from most of the cells lie on the same blue relation line in Fig. 3, which is also the same linear fitting result as that of the gray dots that are derived from the same experimental data in Fig. 2. We can thus confirm that the main collision partners inside most of the cells are He. Figure 3 concerns not only the Cs #2 and Cs #3 cells but also the other eight cells (red dots) examined in 2012 [15] and even one additional cell once used in Ref. [13] (blue dots). The remarkable coincidence of the same FL-R values in Fig. 3 (except for four red data points marked with gray circles) provides us with support in explaining the conundrum raised in our previous experiment [15] and in solving the crisis of secondary standards addressed in Ref. [15]. In our previous experiments, we were perplexed by the fact that the 11 cells (including the Max-Planck-Institute for Quantum Optics (MPQ) cell [13]) yielded randomly scattered "absolute" transition frequencies; in Ref. [15], S. Bergeson pointed out that all glass-cell–based frequency standards were suspicious. In retrospect, this is quite reasonable because the spectral shift and broadening are both uniquely proportional to certain foreign-gas pressures [17,21,22]. To our knowledge, we provide a new transition frequency measured in a high-vacuum cell (black diamond in Fig. 3), which is referred to be the "ultimate absolute frequency" here. "Ultimate" means that all error sources, including atmospheric He, have been excluded. The new linewidth is smaller than those of previous experiments [13–16], and the Lorentzian part is near the calculated value of natural linewidth (920 kHz) [23], as is evidenced in Table 1. Therefore, preparing a highly accurate cell is possible if a high-vacuum cell is used and only requires examination of the "ultimate" linewidth for confidence. Regarding the other four extraordinary data points in Fig. 3, the cells in the two red points, framed by gray circles above the blue FL-R line,

Table 1. Absolute Frequency and Linewidth (Full Width at Half Maximum) of Cs 6S–8S Hyperfine Transitions

Vacuum Cell (2019)		Cell #2 (2017)	Cell #3 (2017)
Frequency Linewidth (F = 4 − 4)	267 (3)[a] 882 (9)[c] (kHz)	345(2)[a] 1085(6)[c] (kHz)	385(2)[a] 1238(13)[c] (kHz)
Frequency Linewidth (F = 3-3)	344 (3)[b] 881(18)[c] (kHz)	421(2)[b] 1108(7)[c] (kHz)	458(2)[b] 1283(12)[c] (kHz)
Cell #4 (2012)		**Cell #2 (2012)**	**Cell #3 (2012)**
Frequency Linewidth (F = 4 − 4)	297(10)[a] 932(11)[c] (kHz)	300(10)[a] 1020(11)[c] (kHz)	338(10)[a] 1150(13)[c] (kHz)

[a] +364, 503, 080, 000 kHz.
[b] +364, 507, 238, 000.
[c] Lorentzian part in "Lorentzian-transit" fitting [15]; see text.

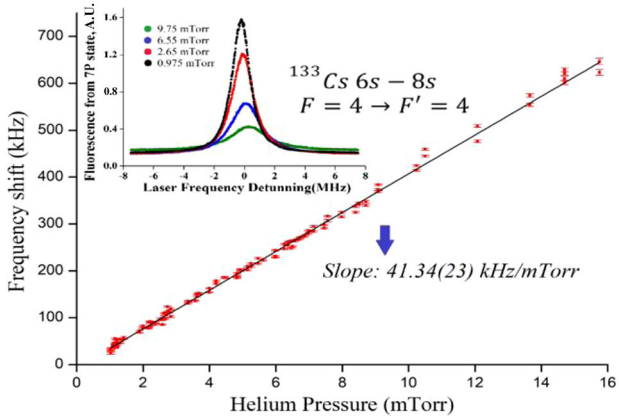

Fig. 2. Frequency-linewidth relation of Cs 6S–8S transition, measured with the He pressure reduced to levels lower than those existent in Earth's atmosphere (error bar is smaller than dot). Top left: typical lineshapes under different He pressures.

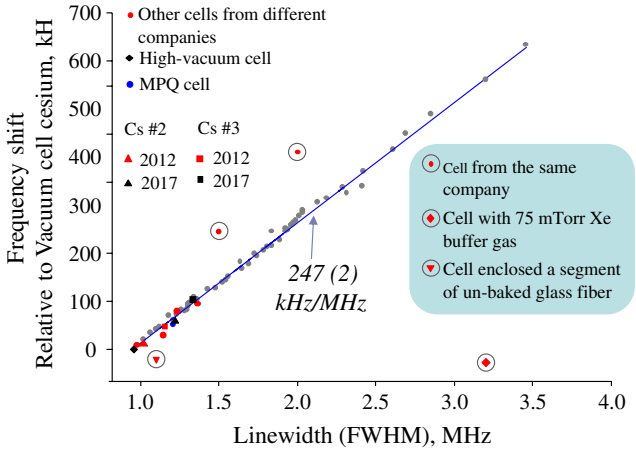

Fig. 3. Frequency-linewidth relation obtained via various experiments; gray color: data from the same experiment as that of displayed in Fig. 2; red color: data taken from the ten cells mentioned in Ref. [15]; blue color: data quoted from Max-Planck-Institute for Quantum Optics (MPQ) work [13]; black color: data taken from Cs #2 and Cs #3 in 2017 and a high-vacuum cell in 2019; gray-circle–marked data are extraordinary (see text).

were purchased from the same company in the same order. We suspect that these two cells were accidently contaminated by a small amount of some unknown gas or by some outgassing due to insufficient baking, such as H_2 molecules; H_2 is another blue shift collision partner in Ref. [22]. The red points framed by gray circles below the blue FL-R line are from cells intentionally made using different treatments to indicate the sensitivity of the 8S-state Cs atom to the environment. That is, the red inverted triangle represents a Cs cell enclosed with a small segment of unbaked glass fiber to demonstrate the influence of normal glass, and the red diamond represents the Cs influenced by the 75 mTorr xenon (Xe). Both of them led to red shift.

All of the previously mentioned measurements could only prove that the contamination of secondary standards is the result of He collision, without clearly indicating the origin of the contamination. Nevertheless, judging from Table 1, we observed that Cs #2 and Cs #3 cells were simultaneously contaminated with the same increasing amount of He, which motivated us to move the Cs #3 cell into the other vacuum chamber and placed Cs cell #2 in another identical optical path for frequency comparison, as shown in Fig. 1. We then filled the chamber with 1.75 atm of He gas to measure the He diffusion coefficient D [24] that is specifically in relation to the dimensions and material of the Cs #3 cell. Through this, we were able to derive the amount of atmospheric He that diffused into Cs #3 during the previous 5 years (discussed later in this Letter). Figure 4 illustrates the first derivative of the frequency shift with respect to time, by which we were able to determine the He diffusion coefficient D of Cs #3. Interestingly, we found that the slope of the FL-R obtained in this experiment, as indicated in the inset of Fig. 4, exhibited precision that was one order of magnitude better than that displayed in Fig. 3. This is because the He pressure was relatively stable during the time of data acquisition in this experiment. The data in Fig. 4 were fitted by the so-called "early time" equation [24] with only two parameters "a" and "b" used in the fitting, that is: $\frac{df(t)}{dt} = \alpha \frac{dP(t)}{dt} = a \times \frac{e^{-\frac{b}{t}}}{\sqrt{t}}$ where $\alpha = 41.34(23)$ kHz/mTorr from the result in Fig. 2; $b = d^2/4D$ with d being the thickness of the cell wall (0.16 cm); a is a function of α, diffusion coefficient D, solubility, the cell dimensions, the surrounding He pressure, and so on. The two constants b and a in Fig. 4 are fitted as 272 (11) and 3.3×10^4 (0.4), respectively. We thus obtained the He diffusion coefficient D of Cs #3 cell as $D = 5.75\ (24) \times 10^{-9}$ cm^2/s at 23°C. This value is in a good agreement with that reported in Ref. [24], in which the value of D of Pyrex 7740 was determined to be 7.74×10^{-9} cm^2/s at 27°C. The value of D and a were then applied to the "late time" [24] equation to extrapolate the amount of He pressure of the Cs #3 cell that had once diffused from the atmosphere, that is

$$P_{5-year} = \frac{2\left(\sqrt{\pi}\right)^3 a h \sqrt{D} P_1}{2(\ln) A \alpha P} (\text{t-c}),$$

where the resulting helium pressure P_{5-year} in cell #3 means that the diffusion time t is set to be 5 years under the condition of 4 mTorr [17] atmospheric helium pressure P_1; R, A, and h are the diameter (2.54 cm), area (89.93 cm^2), and length (10 cm) of the Cs #3 cell, respectively; P is 1.75 atm; c is a function of D as well as the cell dimensions and is negligible here because it was three orders of magnitude smaller than that when t was 5 years. We concluded from these calculations that atmospheric helium could result in P_{5-year} of 1.29 (17) mTorr He pressure inside the Cs #3 cell. We compare this derived He pressure to the experimental results of Fig. 2, we find a remarkable agreement since the 46 kHz shift in Fig. 2 is just corresponding to 1.11 (12) mTorr He collision. That means the helium increment in Cs cell #2, #3 that is displayed in Table 1, from 2012 to 2017, resulted from the atmosphere.

From all the independent experiments reported in this Letter that were performed in different years and using different Cs sources, we conclude that atmospheric He plays a critical role in Cs #2 and Cs #3 contamination and most likely also in that of the other cells in Fig. 3. A high-vacuum-chamber based spectrometer is suggested as a more suitable candidate for secondary optical clocks because a compact dispenser-based vacuum chamber has already been invented, with approximately 1.5 years of operation time per dispenser [25]. Note that he

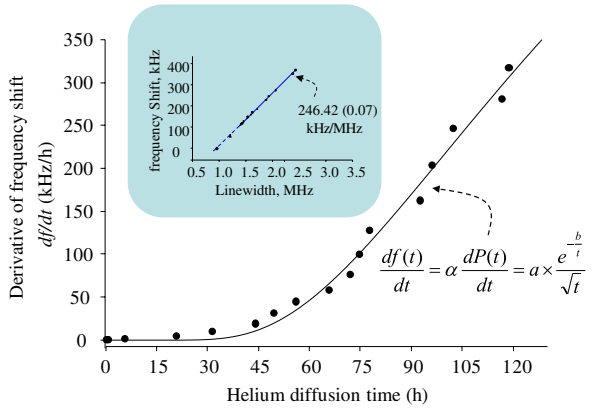

Fig. 4. Experimental data (black circle) taken from the Cs #3 cell surrounded with 1.75 atm He; the data were fitted (black line) by the formula shown on the bottom right [24], see text. Inset: frequency-linewidth relation in this experiment.

collisions would also influence the 6S–6, P–6S two-photon-transition Cs clock (CPT clock) [26]. The findings of this study revealed that the 8S-state Cs atom is an effective indicator of He contamination because its excited valance electron is more weakly bound by nucleon compared with, for example, a Rb atom. In fact, the Cs valence electron possesses the lowest ionization energy on the periodic table, even lower than francium (Fr). This explains why the slope in Fig. 2 is twice that of the Rb 5S–7S two-photon transition [21.0 (6) kHz/mTorr] observed in a previous experiment [17]. If the outgassing from glass is excluded (sufficient baking), our results offer a frequency correction of the Cs 6S–8S frequency standard by merely measuring the linewidth, which assists greatly for maintaining the secondary clock without need of the expensive comb lasers and microwave Cs clock. In other words, the FL-R in the inset of Fig. 4 could be used for precisely judging He contamination, which is the most common alkali cell contamination, as identified in our study.

Funding. Ministry of Science and Technology, Taiwan (MOST 108-2112-M-008-012).

Acknowledgment. The authors are indebted to Dr. Jon Hougen in National Institute of Standards and Technology (USA) for his trust that "atmospheric" helium played a critical role in our previous spectrum and for offering us encouragement to pursue the truth. Dr. Hougen suddenly passed away during the time of preparing this paper. We thank Dr. Ying-Cheng Chen for suggesting the use of a high-vacuum cell for the ultimate determination of cesium transition frequency. Dr. Jim Ming Lin in Institute of Atomic and Molecular Science (Taiwan) kindly supported us by providing a pumping station. We are also grateful to Chunghwa Telecom Laboratories for providing a cesium atomic clock.

Disclosures. The authors declare no conflicts of interest.

REFERENCES AND NOTES

1. F. Riehle, Nat. Photonics **11**, 25 (2017).
2. S. Knappe, V. Shah, P. D. D. Schwindt, L. Hollberg, J. Kitching, L. A. Liew, and J. Moreland, Appl. Phys. Lett. **85**, 1460 (2004).
3. R. Felder, Metrologia **42**, 323 (2005).
4. http://www.bipm.org/en/publications/mises-en-pratique/standard-frequencies.html and references therein.
5. K. W. Martin, G. Phelps, N. D. Lemke, M. S. Bigelow, B. Stuhl, M. Wojcik, M. Holt, I. Coddington, M. W. Bishop, and J. H. Burke, Phys. Rev. Appl. **9**, 014019 (2018).
6. C. S. Edwards, G. P. Barwood, H. S. Margolis, P. Gill, and W. R. C. Rowley, Metrologia **42**, 464 (2005).
7. D. Touahri, O. Acef, A. Clairon, J. J. Zondy, R. Felder, L. Hilico, B. de Beauvoir, F. Biraben, and F. Nez, Opt. Commun. **133**, 471 (1997).
8. H. C. Chui, M. S. Ko, Y. W. Liu, J. T. Shy, J. L. Peng, and H. Ahn, Opt. Lett. **30**, 842 (2005).
9. A. Marian, M. C. Stowe, D. Felinto, and J. Ye, Phys. Rev. Lett. **95**, 023001 (2005).
10. K. Pandey, P. V. Kiran Kumar, M. V. Suryanarayana, and V. Natarajan, Opt. Lett. **33**, 1675 (2008).
11. P. Morzyński, P. Wcisło, P. Ablewski, R. Gartman, W. Gawlik, P. Masłowski, B. Nagórny, F. Ozimek, C. Radzewicz, M. Witkowski, R. Ciuryło, and M. Zawada, Opt. Lett. **38**, 4581 (2013).
12. I. Barmes, S. Witte, and K. S. E. Eikema, Phys. Rev. Lett. **111**, 023007 (2013).
13. P. Fendel, S. D. Bergeson, T. Udem, and T. W. Hansch, Opt. Lett. **32**, 701 (2007).
14. G. Hagel, C. Nesi, L. Jozefowski, C. Schwob, F. Nez, and F. Biraben, Opt. Commun. **160**, 1 (1999).
15. C. M. Wu, T. W. Liu, M. H. Wu, R. K. Lee, and W. Y. Cheng, Opt. Lett. **38**, 3186 (2013).
16. C. M. Wu, T. W. Liu, and W. Y. Cheng, Phys. Rev. A **92**, 042504 (2015).
17. N. D. Zameroski, G. D. Hager, C. J. Erickson, and J. H. Burke, J. Phys. B **47**, 225205 (2014).
18. Symmetricom 5071a Cs clock, whose frequency was traced to UTC (Coordinated Universal Time) via the flying clock method and that resulted in 1.4×10^{-14} one-day accuracy and 10^{-11} for 10 second sampling time.
19. F. Biraben, M. Bassini, and B. Cagnac, J. Phys. (France) **40**, 445 (1979).
20. Edwards Inc. with model: WRG-S-DN40CF. The gauge reading has been corrected for He by nitrogen molecule, that is, reading correction fact 1.05 at our vacuum range.
21. W. Demtroder, *Laser Spectroscopy: Basic Concepts and Instrumentation*, 3rd ed. (Springer, 2003).
22. N. Allard and J. Kielkopf, Rev. Mod. Phys. **54**, 1103 (1982).
23. A. Sieradzan, M. D. Havey, and M. S. Safranova, Phys. Rev. A **69**, 022502 (2004).
24. W. A. Rogers, R. S. Buritz, and D. Alpert, J. Appl. Phys. **25**, 868 (1954).
25. E. M. Bridge, J. Millen, C. S. Adams, and M. P. A. Jones, Rev. Sci. Instrum. **80**, 013101 (2009).
26. P. J. Oreto, Y. Y. Jau, A. B. Post, N. N. Kuzma, and W. Happer, Phys. Rev. A **69**, 042716 (2004).

140.113.38.39 {ts '2020-07-15 01:51:47'}